Friction Stir Welding and Processing V
Edited by: Rajiv S. Mishra, Murray W. Mahoney, and Thomas J. Lienert
TMS (The Minerals, Metals & Materials Society), 2009

AMICROSTRUCTURE – PROCESSING RELATIONSHIPS IN FRICTION STIR PROCESSING (FSP) OF NiAl BRONZE

Terry R McNelley[1], Srinvasan Swaminathan[2], Jianqing Su[1] and Sarath Menon[1]

[1]Naval Postgraduate School
Department of Mechanical and Astronautical Engineering
Monterey, CA 93943-5146
[2]GE Global Research
Bangalore, Karnataka 560066 India

Keywords: Friction stir processing; Multi-pass processing; Microstructure; Strain distribution; NiAl bronze

Abstract

The evolution of SZ and thermomechanically affected zone (TMAZ) microstructures during single-pass and multi-pass FSP by rectangular and spiral raster processes will be summarized. Microstructures produced by thermomechanical simulations will be compared to those produced during FSP. The distortion of microstructure constituents in thermomechanical simulations may be applied to estimation of SZ and TMAZ strain distributions in the initial FSP pass. Recrystallization in the primary α constituent is initiated at κ_{iv} (Fe_3Al) particles prior to their dissolution during straining.

Introduction

An allied process of friction stir welding[1] (FSW), friction stir processing (FSP) is emerging as a novel metal working technology that can provide localized modification and control of microstructures in near-surface layers of processed components[2-4]. In FSP, a cylindrical, wear-resistant tool consisting of a smaller diameter pin with a concentric, larger diameter shoulder is rotated and forced into a surface of the work piece. As the tool pin penetrates, a combination of frictional and adiabatic heating softens the material so that tool rotation induces a stirring action and flow of material about the pin. Severe but localized plastic deformation results in formation of a stir zone (SZ) while adjacent regions experience only moderate straining and comprise the thermomechanically affected zone (TMAZ). The tool shoulder prevents upward flow of material and serves to forge the SZ as it comes in contact with the work piece surface; large areas may then be processed by traversing the tool in a pattern on the work piece surface.

Traversing patterns in FSP have included repeated linear traverses that are offset from one another by a characteristic step-over distance. Raster and rectangular or circular spiral patterns have also been employed wherein successive traverses are, again, offset by a characteristic step over distance. In FSP, the step-over distance is an important process parameter in addition to the tool rpm and traversing rate. When the step-over distance is smaller than the minimum diameter of the tool pin successive passes will overlap one another and FSP inherently becomes a mult-stage process.

FSP has been employed to homogenize and refine microstructures in both cast and wrought metals including alloys of Al[5-10] and Mg[11,12] and higher melting alloys of Cu[13], Fe[14] and Ti[15]. Benefits of FSP in cast metals include the elimination of porosity and local conversion of

Report Documentation Page

Form Approved
OMB No. 0704-0188

1. REPORT DATE	2. REPORT TYPE	3. DATES COVERED
FEB 2009		**00-00-2009 to 00-00-2009**

4. TITLE AND SUBTITLE	5a. CONTRACT NUMBER
A Microstructure - Processing Relationships in Friction Stir Processing (FSP) of NiAl Bronze	5b. GRANT NUMBER
	5c. PROGRAM ELEMENT NUMBER
6. AUTHOR(S)	5d. PROJECT NUMBER
	5e. TASK NUMBER
	5f. WORK UNIT NUMBER
7. PERFORMING ORGANIZATION NAME(S) AND ADDRESS(ES) **Naval Postgraduate School,Department of Mechanical and Astronautical Engineering,Monterey,CA,93943-5146**	8. PERFORMING ORGANIZATION REPORT NUMBER
9. SPONSORING/MONITORING AGENCY NAME(S) AND ADDRESS(ES)	10. SPONSOR/MONITOR'S ACRONYM(S)
	11. SPONSOR/MONITOR'S REPORT NUMBER(S)

12. DISTRIBUTION/AVAILABILITY STATEMENT
Approved for public release; distribution unlimited

13. SUPPLEMENTARY NOTES
See also ADM002300. Presented at the Minerals, Metals and Materials Annual Meeting and Exhibition (138th)(TMS 2009) Held in San Francisco, California on February 15-19, 2009. Sponsored in part by the Navy.

14. ABSTRACT
The evolution of SZ and thermomechanically affected zone (TMAZ) microstructures during single-pass and multi-pass FSP by rectangular and spiral raster processes will be summarized. Microstructures produced by thermomechanical simulations will be compared to those produced during FSP. The distortion of microstructure constituents in thermomechanical simulations may be applied to estimation of SZ and TMAZ strain distributions in the initial FSP pass. Recrystallization in the primary constituent is initiated at iv (Fe3Al) particles prior to their dissolution during straining.

15. SUBJECT TERMS

16. SECURITY CLASSIFICATION OF:			17. LIMITATION OF ABSTRACT	18. NUMBER OF PAGES	19a. NAME OF RESPONSIBLE PERSON
a. REPORT **unclassified**	b. ABSTRACT **unclassified**	c. THIS PAGE **unclassified**	**Same as Report (SAR)**	**8**	

the as-cast microstructure to a wrought condition in the absence of macroscopic shape change. Cast NiAl bronze alloys are used for components in a wide range of marine applications due to good combinations of corrosion resistance strength, toughness, friction coefficients and non-sparking behavior. Many cast components are large and resulting slow cooling rates contribute to coarse microstructures and reduced physical and mechanical properties. In such circumstances NiAl bronze materials may not be readily heat treatable and, so, FSP represents an alternative means of selectively strengthening the surfaces of such components. However, the full benefit of FSP will only be realized when tool design and process parameters are selected to achieve uniform deformation and homogeneous microstructures throughout the SZ. The present work will illustrate a comparison of SZ microstructures after an initial FSP pass and following multi-pass FSP. The SZ microstructure is inhomogeneous after the initial pass, with some locations exhibiting features suggestive of only modest deformation (von Mises strains $\leq$3.0). Thermomechanical simulations have been conducted and analyzed to assess the distribution of local strains in the vicinity of the tool during the initial pass.

Experimental

Two plates, each approximately 300mm × 152mm × 42mm in thickness, were sectioned from a large NiAl bronze casting. Composition data for the alloys of these plates are included in Table I. Details of the alloy constitution of as-cast material as well as the effect of FSP on microstructure have been given previously. The FSP was conducted using a tool fabricated in Densimet® and

Table I. Compositions (in wt. pct.) of the NiAl bronze alloy in this investigation

Element	Cu	Al	Ni	Fe	Mn	Si	Pb
Min-max	(min)79.0	8.5-9.5	4.0-5.0	3.5-4.5	0.8-1.5	0.10(max)	0.03(max)
Nominal	81	9	5	4	1	-	-
Alloy	81.2	9.39	4.29	3.67	1.20	0.05	<0.005

having a pin in the shape of a truncated cone 12.7mm in length, a base diameter of 15mm, and tip diameter of 6.3mm. The pin also had a step-spiral thread feature. All processing was conducted at 1200rpm and a traversing rate of 51mm min^{-1}.In order to examine the microstructure corresponding to an initial pass, a single linear FSP traverse was made. The traverse was approximately 250mm in length and centered along the long dimension of one of the plates. Multi-pass FSP was conducted on the other plate using a rectangular spiral pattern. Processing was initiated with a 200mm traverse centered along the long dimension of the plate. A spiral pattern was followed with the advancing side of the tool to the outside of the pattern and with a step-over distance of 4.5mm. Separately, cylindrical samples 11.1mm in diameter and 25.4mm in length were prepared and subjected to hot compression in a Gleeble® thermomechanical simulator. For the current investigation, a sample was heated to 900°C, held for 2mins, then compressed to a true strain of 0.58 at a displacement rate of 200mm s^{-1} and, finally, cooled to ambient at ~7°Cs^{-1}.

Samples for optical microscopy were prepared either by sectioning on a transverse plane or on the plane of the plan view after FSP of the plates. A sample from the hot compression test was sectioned to reveal the plane containing the compression axis. Transverse views of the SZ in both of the FSP plates were sectioned from locations near the middle of the processed region and correspond to a steady state. The plan view sample was sectioned from the pin tool extraction site for the single traverse at the mid-depth of the stir zone. Optical microscopy sample preparation procedures have been given previously. Etched samples from the hot compression material were also examined using secondary imaging in a Topcon S510 scanning electron microscope operating at 15kV.

Results

The Initial FSP Pass

A montage of images illustrating the microstructure of a transverse section through the SZ after a single FSP pass is shown in Fig. 1. The tool pin profile is superimposed on the image in Fig. 1; the advancing side (tool rotation and travel directions are the same) is to the right, and retreating side (indicated by Rt in the image; tool rotation and travel directions are opposite) is to the left. The SZ microstructure is internally inhomogeneous and the surrounding microstructures reflect

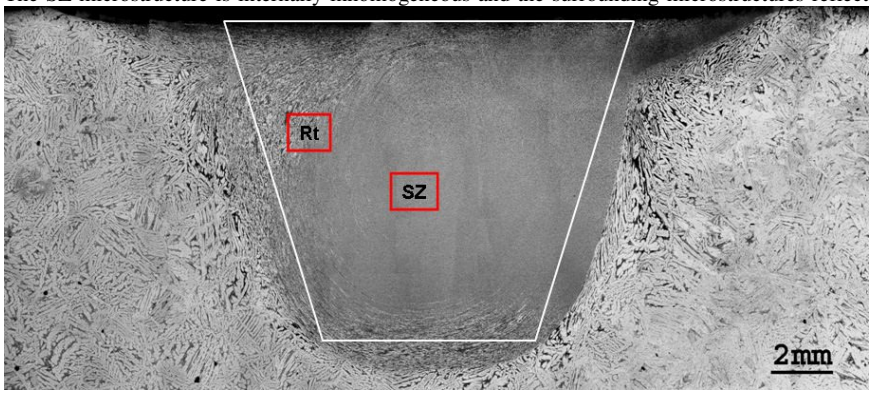

Fig. 1. A montage of images showing the microstructure of a transverse section through the SZ after a single FSP pass; the tool pin profile is superimposed on the image.

asymmetric deformation from the advancing to the retreating side of the tool. The advancing side interface with the base metal is distinct while the interface is more diffuse under the tool and on the retreating side. The heating portion of the FSP thermomechanical cycle results in the eutectoid reversion reaction $\alpha + \kappa_{iii} \rightarrow \beta$ in locations where the temperature, T, is $\geq 800°C$, the eutectoid temperature in the quasi binary formed by the α and κ_{iii} phases in the Cu-Al-Ni ternary[16-20]. The dark-etching constituent in the TMAZ is the cooling transformation product of this β. This transformation product embrittles the heat affected zone of fusion welds as well as the TMAZ following FSP of as-cast NiAl bronze. The light-etching constituent is the undissolved primary α. The α and β have deformed in a compatible manner in many locations around the SZ periphery and TMAZ; the distortion of these constituents results in a layer appearance of the structure and suggests that they are pulled upward along the Rt side from under and then across the upper portion of the SZ as they experience moderate deformation. In contrast the central portion of the SZ appears to be much more highly refined and details of the structure are not discernable at this magnification. The layered arrangement of the primary α and β transformation product is apparent at higher magnifications in the micrographs of Fig. 2(a) and (b), which are from the location denoted Rt in Fig. 1. Recrystallization is apparent within the primary α in the microsgraph of Fig. 2(b), although this constituent remains separate and distinct in this location. In the central regions of the SZ, shown in Fig. 2(c), the layered structure is no longer apparent, suggesting that the α + β mixture became fragmented, likely due to much larger local strains during FSP.

Multi-Pass FSP

A montage of images from the SZ in the plate subjected to multi-pass FSP is shown in Fig. 3(a) wherein pin tool profiles are superimposed for two successive passes. These profiles show that all SZ locations experience deformation from at least two passes, and more than two passes in

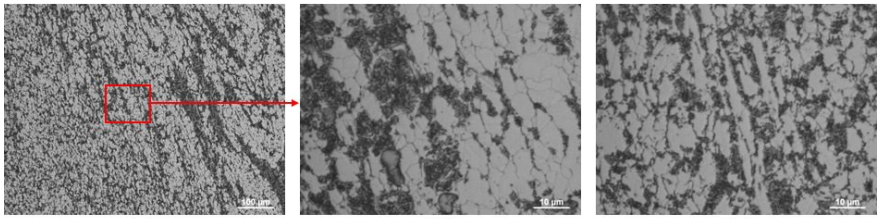

Fig. 2. Higher magnification micrographs of the region denoted Rt in Fig. 1 are shown in (a) and (b), illustrating the layered nature of the microstructure. A more homogeneous microstructure is apparent in the center of the SZ shown in (c).

the upper regions of the SZ. In general, the microstructure is more uniform throughout the SZ volume although some locations in the lower SZ exhibit flow lines indicative of moderately deformed material from beneath the SZ that is being pulled upward by the pin tool rotation. The micrograph in Fig. 3(b) is from the location indicated in Fig. 3(a) and shows a representative example of this SZ at a higher magnification. At this location the microstructure comprises 5 - 8μm primary α grains and discrete, irregularly shaped regions of β transformation products. Thus the additional deformation induced by overlapping passes increases strains and homogenizes and refines the structure throughout the SZ.

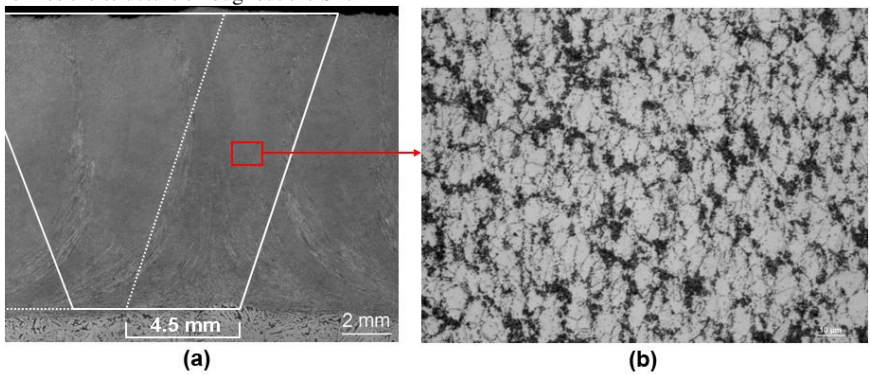

Fig. 3. A montage of images of the stir zone for multi-pass FSP is shown in (a) and overlap the the pin tool profiles is illustrated by the solid and dotted lines. A microstructure that is representative of the SZ is shown in (b) and consists of refined grains of α and dispersed β transformation products.

Estimation of Strains during FSP

Quantitative analysis of single-pass microstructures has been employed to estimate peak SZ temperatures and their distribution[16-20]. Values obtained from these estimates are 900 – 1000°C and direct thermocouple measures have subsequently confirmed the validity of these estimates. While numerous micrographs showing TMAZ and SZ grain distortion have appeared in the literature there have been no reported attempts to quantify the corresponding strains. An example illustrating strains and strain gradients in the vicinity of the tool extraction site for material subjected only to the initial FSP pass in this investigation is shown in Fig. 4. This montage of

images was obtained from a plan view of a location at the mid-depth of the SZ. Ahead of the tool (the upper micrograph) the onset of straining is reflected in the shearing distortion of the primary and eutectoid constituents in a direction tangential to the surface of the tool and in the direction of tool rotation. In this location the distortion extends outward a distance of ~400μm, and a distinct gradient in strain is also evident over this distance. The grain distortion on either side of the tool extends outward much farther (~1mm) than it does ahead of the tool. The reflects the backward tilt of the tool by ~3° such that the influence of the tool shoulder is greater to the sides of the tool than it is ahead of the tool. At this depth in the SZ, the microstructure behind the tool corresponds to the very fine grain structure evident at the mid-depth of the SZ in Fig. 1.

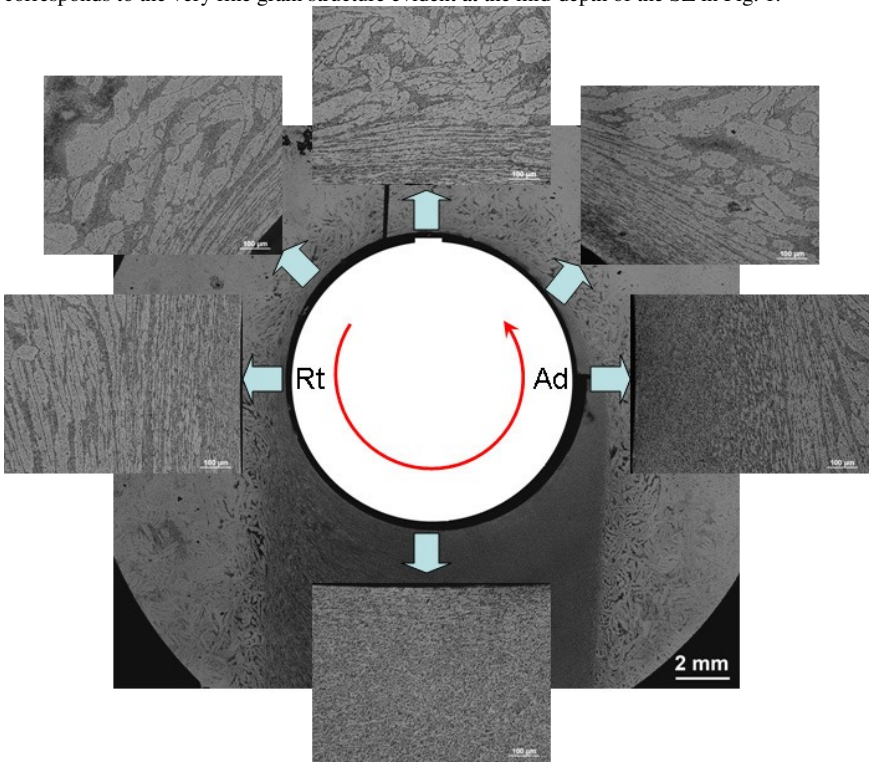

Fig. 4. A montage of images from the tool extraction site for a single FSP pass; these images were acquired for the plan view and from the mid-depth of the stir zone, and illustrate the varying gradient in strain around the tool pin.

The two constituent (primary α and β) apparently deform compatibly during FSP and retain their identity to moderate strains and during subsequent cooling. Fig. 5 shows two secondary images from scanning electron microscopy examination of a NiAl bronze sample heated to 900°C and then compressed to a nominal strain of 0.54 in a Gleeble thermomechanical simulator. At a higher magnification in Fig. 5(a), recrystallization accompanies deformation. This is apparent in the presence of annealing twins formed after the recrystallzation event as well as in the decoration of grain boundaries by precipitation of fine particles, which likely are the κ_{iv} (Fe_3Al)

phase, upon cooling after deformation. At a lower magnification, the flattening of the originally ellipsoidal primary α grains is evident. These grains are embedded in transformation products of the β, which also deformed during the compression at 900°C. As indicated in the schematic

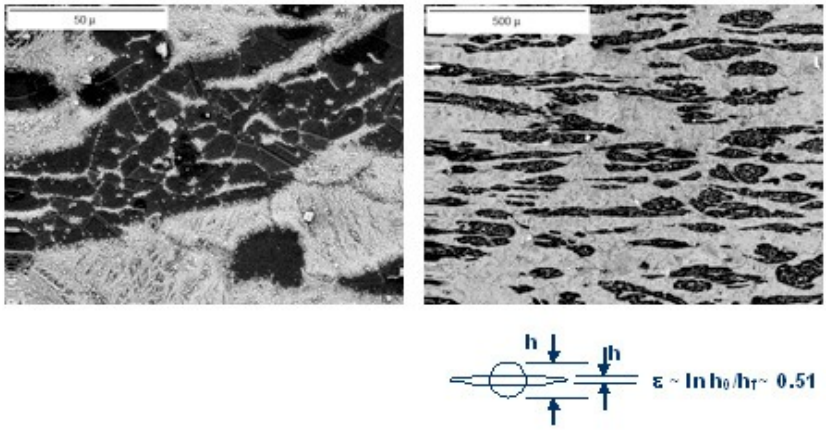

Fig. 5. Secondary SEM images from a sample deformed to a strain of 0.54 by Gleeble thermomechanical simulation and showing recrystallization in the primary α in (a) and that the distortion of the constituent may employed to estimate strains in the TMAZ.

below the microsgraph, a value of strain may be estimated by analysis of the distortion of the primary α; the value obtained at this location ($\varepsilon \cong 0.51$) corresponds closely to the compressive strain applied to the sample ($\varepsilon_{app} \cong 0.54$). An application of such measurements to the strain field ahead of the pin tool is illustrated in Fig. 6. Direct temperature measurements from a thermocouples embedded in a location incorporated into the SZ of an NiAl bronze plate subjected to FSP are shown at the left. The portion of the overall plot of temperature as a function of time that corresponds to the extent of region ahead of the tool examined metallographically is shown in this plot. Quantitative microscopy measurements of the volume fraction of β transformation products as well as strain estimates from the distortion of the primary α are summarized in the plot to the right in Fig. 6. The volume fraction of β is ~0.2 in as cast NiAl bronze (this is the volume fraction of the lamellar eutectoid constituent after equilibrium cooling at rates of ~10^{-3} °Cs^{-1}). As the tool approaches, the volume fraction of β transformation products increases as β forms upon heating and is then retained at the higher cooling rates characteristic of FSP (10 – 100°Cs^{-1}). Simultaneously, the estimated strain values increases, reflecting the distortion of the primary α constituent. Clearly, the onset of straining has the effect of greatly accelerating the forward transformation $\alpha + \kappa_{iii} \rightarrow \beta$; this likely reflects the generation of excess vacancies during the severe deformation of the material[21-23]. Local strain estimates by this method suggests that von Mises equivalent strains up to about 3.0 are encountered at a distance of ~100µm ahead of the tool pin. In future work this approach will be taken to estimation of local strains at several locations around the tool in a attempt to characterize the entire deformation field during FSP.

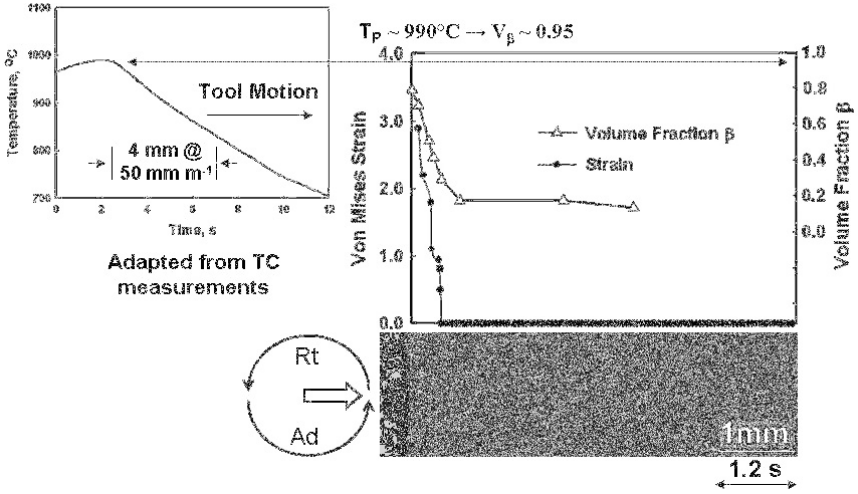

Fig. 6. Direct thermocouple measurements of SZ temperature[17] are plotted at the upper left; corresponding evaluations of volume fraction of β are plotted at the right[16,18,19] and compared to measurements of the strain from distortion of the primary α. Concurrent straining accelerates the reversion of the eutectoid so that the volume fraction of β approaches the equilibrium value (0.95) for the measured local peak temperature(990°C).

Conclusions

The following conclusions may be drawn from this work:

- Straining is non-uniform in the initial pass of FSP and SZ microstructures are inhomogeneous. Some locations may reflect local von Mises strains that are ≤1.0.
- With a small step-over distance such that the pin tool profile overlaps on successive pass a uniform and homogeneous SZ microstructure can be achieved.
- The strain distribution about the tool pin is complex and reflects effects of both the tool pin and tool shoulder.
- The distortion of the primary α may be employed as a means to estimate local strains in locations surrounding the tool.
- Estimates of the strain from shape change of microstructure constituents in FSP of NiAl bronze suggest that the local von Mises strain values are ≤3.0 at many SZ locations.
- Control of step-over distance in multi-pass FSP is required to impart uniform and homogeneous strains and obtain optimum SZ microstructures and mechanical properties.

References

1. W.M. Thomas, E.D. Nicholas, J.C. Needham, M.G. Murch, P. Templesmith and C.J. Daws: G.B. Patent Application No. 9125978.8, December, 1991; U.S. Patent No. 5460317, October, 1995
2. R.S. Mishra: *Advanced Materials and Processes*, 2003, vol. 161(10), pp. 43-46
3. R.S. Mishra, Z.Y. Ma and I. Charit: *Mater. Sci. Engng. A*, 2003, vol. A341, pp. 307-10

4. Z.Y. Ma, R.S. Mishra and M. W. Mahoney: in *Friction Stir Welding and Processing II*, K.V. Jata, M.W. Mahoney, R.S. Mishra, S.L. Semiatin and T. Lienert, eds., TMS, Warrendale, PA, 2003, pp. 221-30
5. R.S. Mishra, M.W. Mahoney, S.X. McFadden, N.A. Mara and A.K. Mukherjee: *Scripta Mater.*, 2000, vol. 42, pp. 163-68
6. R.S. Mishra and M.W. Mahoney: in *Superplasticity in Advanced Materials – Proceedings of ICSAM2000*, N. Chandra, ed., Materials Science Forum, Trans Tech Publications, Switzerland, 2001, vol. 357-59, pp. 507-14
7. Z.Y. Ma, R.S. Mishra and M.W. Mahoney: *Acta Mater.*, 2002, vol. 50, pp. 4419-30
8. I. Charit and R.S. Mishra: *Mater. Sci. Eng. A*, 2003, vol. A359, pp. 290-96
9. Z.Y. Ma, R.S. Mishra M.W. Mahoney and R. Grimes: *Mater. Sci. Engng. A*, 2003, vol. A351, pp. 148-53
10. Y.S. Sato, M. Urata and H. Kokawa: *Metal. Mater. Trans. A*, 2002, vol. 33A, pp. 625-635
11. S.H.C. Park, Y.S. Sato and H. Kokawa: *Scripta Mater.*, 2003, vol. 49, pp. 161-6
12. D. Zhang, M. Suzuki and K. Maruyama: *Scripta Mater.*, 2005, vol. 52, pp. 899-903
13. H.S. Park, T. Kimura, T. Murakami, Y. Nagano, K. Nakata and M. Ushio: *Mater. Sci. Eng. A*, 2004, vol. A371, pp. 160-169
14. Y.S. Sato, T.W. Nelson and C.J. Sterling: *Acta Mater.*, 2005, vol. 53, pp. 637-45
15. A.P. Reynolds, E. Hood and W. Tang: *Scripta Mater.*, 2005, vol. 52, pp. 491-4
16. K. Oh-ishi, A. P. Zhilyaev, R. Williams and T. R. McNelley: in *Friction Stir Welding and Processing III*, K.V. Jata, M.W. Mahoney, R.S. Mishra and T.J. Lienert, eds., TMS, Warrendale, PA, 2005, pp. 107-14
17. T.R. McNelley, K. Oh-ishi and A. P. Zhilyaev: in *Processing and Manufacturing of Advanced Materials – Proceedings of THERMEC'2006*, T. Chandra, K. Tsuzki, M. Militzer and C. Ravichandran, eds., Materials Science Forum, Trans Tech Publications, Switzerland, 2007, vols. 539 – 43, pp. 3745-50
18. K. Oh-ishi and T.R. McNelley: *Metall. Mater. Trans. A*, 2004, vol. 35A, pp. 2951-61
19. K. Oh-ishi and T.R. McNelley: *Metall. Mater. Trans. A*, 2005, vol. 36A, pp. 1575-85
20. K. Oh-ishi, A.P. Zhilyaev and T.R. McNelley: *Metall. Mater. Trans. A*, 2006, vol. 37A, pp. 2239-51
21. J.L. Robbins, O.C. Shepard and O.D. Sherby: *J. Iron Steel Inst.*, 1964, vol. 202, pp. 804-7
22. O.D. Sherby, B. Walser, C.M. Young and E.M. Cady: *Scripta Metall.*, 1975, vol. 9, pp. 569-74
23. B. Walser and O.D. Sherby: *Metall. Trans. A*, 1979, vol. 10A, pp. 1461-71